Available online at www.sciencedirect.com

ScienceDirect

www.elsevier.com/locate/jes

JES JOURNAL OF ENVIRONMENTAL SCIENCES

www.jesc.ac.cn

Application of a hybrid gravity-driven membrane filtration and dissolved ozone flotation (MDOF) process for wastewater reclamation and membrane fouling mitigation

Xin Jin[1], *Wei Wang*[1], *Shuai Wang*[1], *Pengkang Jin*[1,*], *Xiaochang C. Wang*[1], *Wushou Zhang*[2], *Weijun An*[2], *Yong Wang*[1]

1. *Key Lab of Northwest Water Resource, Environment and Ecology, MOE, Xi'an University of Architecture and Technology, Xi'an 710055, China*

2. *Langzheng Environmental Protection Technology Co., Ltd., Xi'an 710075, China*

ARTICLE INFO

Article history:
Received 17 October 2018
Revised 11 February 2019
Accepted 13 February 2019
Available online 23 February 2019

Keywords:
Dissolved ozone flotation
Gravity-driven membrane filtration
Membrane fouling
In situ ozonation

ABSTRACT

This study proposed a novel membrane filtration and dissolved ozone flotation integrated (MDOF) process and tested it at pilot scale. Membrane filtration in the MDOF process was operated in gravity-driven mode, and required no backwashing, flushing, or chemical cleaning. Because ozone was added in the MDOF process, ozonation, coagulation, and membrane filtration could occur in a single reactor. Moreover, *in situ* ozonation occurred in the MDOF process, which differs from the conventional pre-ozonation membrane filtration process. Significant enhancement of turbidity removal was further achieved through the addition of membrane filtration. Membrane fouling was mitigated in the MDOF process compared to the MDAF process. *In situ* ozonation in the MDOF process decreased the fluorescence intensity and transformed the high MW dissolved organics into small MW compounds. For the fouling layer, the extracellular polymeric substance (EPS) contents and cake layer morphology were analyzed. The results indicated that the contents of EPS decreased. Furthermore, a thinner and more loosely structured cake layer formed in the MDOF process. Because coagulation and ozonation occurred simultaneously in a single reactor, the generation of hydroxyl radicals was enhanced through the catalytic effect of Al-based coagulants on ozone decomposition, which further alleviated membrane fouling in the MDOF process.

Introduction

Dissolved air flotation (DAF) is a clarification technology used for removing low density particles from water (Edzwald, 2010). However, DAF exhibits limited removal performance for dissolved organic matter (DOM). To enhance DOM removal, the addition of ozone instead of air was applied, and dissolved ozone flotation (DOF) was proposed (Jin et al., 2006; Jin et al., 2016; Lee et al., 2004). DOF is an innovative water treatment process that combines ozonation and flotation (Jin et al., 2015). Compared with the

* *Corresponding author. E-mail:* pkjin@hotmail.com. (Pengkang Jin).

https://doi.org/10.1016/j.jes.2019.02.011
1001-0742 © 2019 The Research Center for Eco-Environmental Sciences, Chinese Academy of Sciences. Published by Elsevier B.V.

conventional tertiary wastewater treatment process, which comprises coagulation, sedimentation, and filtration, the DOF process is superior in terms of decolorization and the removal of odors and organic matter (Jin et al., 2015).

The DAF process can be used as a pretreatment step for membrane filtration and is usually placed horizontally, in-line with the membrane filtration process (Edzwald, 2010). In to our previous study, the DOF process that was developed had a vertical configuration (Jin et al., 2006; Jin et al., 2015). In addition, purified water was collected from the bottom part of the reactor. Therefore, it is possible to design a gravity-driven membrane (GDM) filtration system to make full use of the water pressure-head if the membrane module can be placed at the base of the reactor. In the GDM filtration process, the microfiltration (MF)/ultrafiltration (UF) membrane is located 40–100 cm below the water level (*i.e.*, at a hydrostatic pressure of 40–100 mbar) (Fortunato et al., 2016; Wu et al., 2017). Compared to conventional pressurized or vacuum-driven MF/UF processes, the GDM filtration process is free of the need for chemical cleaning and has extremely low energy consumption (Ma et al., 2017; Wu et al., 2016).

Membrane fouling is an inevitable impediment, limiting the membrane performance and the application of MF/UF, which causes a reduction in permeation flux, an increase in filter resistance, and the need for more frequent physical/chemical cleaning (Chang et al., 2015; Wang et al., 2017a; Zheng et al., 2014). Several approaches have been proposed for mitigating membrane fouling, including ozonation (Cheng et al., 2016; Geluwe et al., 2011; Xue et al., 2016) and coagulation (Huang et al., 2018; Wang et al., 2018). Compared with the DAF process, ozone is introduced instead of air to enhance the oxidation ability. However, little is known about the effect of ozone addition on GDM filtration in the DOF process.

In most cases, ozone has been dosed in a pre-ozonation mode, which requires an extra tank for ozone to come in contact with the water flow (Huang et al., 2009). The application of pre-ozonation can mitigate membrane fouling, as ozone can oxidize DOM to lower molecular weight (MW) substances and can change the molecular structure and hydrophilic proportion of DOM (Kim et al., 2009; Song et al., 2017). However, it was reported that pre-ozonation could not mitigate irreversible fouling caused by the formation of a gel layer on the membrane surface and the blockage of membrane pores that occurs during the filtration process (Lee et al., 2014). To overcome this problem, an innovative method that causes oxidation to occur inside the membrane pores was proposed to further alleviate or even stop fouling *in situ* (Zhang et al., 2013). Direct molecular ozone oxidation and hydroxyl radical oxidation of the feed and foulants deposited on membrane surfaces and within membrane pores were reported to be the main mechanisms for mitigating membrane fouling *in situ* through ozonation (Song et al., 2017; Szymanska et al., 2014). In the DOF process, ozone is dissolved in water and released in the DOF reactor. Therefore, the ozonation occurs *in situ* and is integrated with membrane filtration (Jin et al., 2015). It is of interest to investigate the removal and fouling performance of the integrated membrane filtration and DOF process (MDOF). There is also limited information related to the effect of *in situ* ozonation on GDM filtration.

The aim of this study was to investigate the removal performance of the MDOF process using a pilot scale reactor fed by secondary effluent from a local domestic WWTP. Furthermore, the characteristics of membrane fouling in the MDOF process were also analyzed at different ozone dosages to better understand the alleviation of membrane fouling. This study can facilitate the application of the MDOF process as an alternative wastewater reclamation process.

1. Materials and methods

1.1. *Experimental setup and operating conditions*

A schematic illustration of the experimental setup is given in Fig. 1. The capacity of the experimental setup is 1.5 m^3/hr. The MDOF process integrates dissolved ozone flotation (DOF) and membrane filtration together in a single reactor. The major component of the MDOF reactor is a closed cylindrical compartment with an inner column at the center, thus dividing the cylindrical space into a contact zone and a separation zone. There are two inlets at the bottom of the contact zone. One inlet serves as an entrance for the raw water, *i.e.*, the secondary effluent, after mixing with an 80 mg/L dosage of coagulant (polyaluminum chloride, PAC) through an online hydraulic mixer. The second inlet is the entrance for recycled flow (40% recycling rate) with dissolved ozone. The two flows are well mixed hydraulically in the contact zone. Because of the sharp pressure decrease, micro-ozone bubbles are released at the entrance of the contact zone. Therefore, a contact reaction of ozone with pollutants and the attachment of pollutants onto micro-size ozone bubbles occurs and forms floc-bubble-aggregates at the same time in the contact zone. Water carrying the suspension of floc-bubble-aggregates, free bubbles, and unattached floc particles flows to the separation zone. Here, free bubbles and floc-bubble-aggregates can rise to the surface of the reactor to form the float layer. The sludge of the float layer is collected on the top of the reactor and discharged periodically. Part of the clarified water is further filtered by two flat sheet PVDF micro-filtration membranes (SINAP, pore size: <0.1 μm, effective area: 0.1 m^2) positioned at the bottom of the separation zone. The total height of the tested MDOF reactor was 3.0 m, with a diameter of 0.78 m. Therefore, the membrane filtration could be operated in gravity-driven mode. The rest of the treated water was withdrawn from the bottom of the separation zone. A magnetic valve was installed on the treated water pipe, which was automatically controlled by a time controller so that it could be switched to “open” and “closed” at pre-set time intervals. As the valve opened, treated water flowed out of the MDOF reactor at a regular rate. As the valve closed, the treated water flow was shut down, and the water level began to rise in the MDOF reactor. Thus, sludge in the float layer accumulated on the top could be discharged. Both the residual gas during normal operation and the residual gas along with the discharged sludge in the sludge tank can be collected into the ozone destructor. In the MDOF reactor, ozone gas was generated by an ozone generator (CF-G-2-50g, GUOLIN, China) and dissolved in recycled water using an ozone dissolving pump (20NPD04Z, Nikuni, Japan), followed by a saturator that

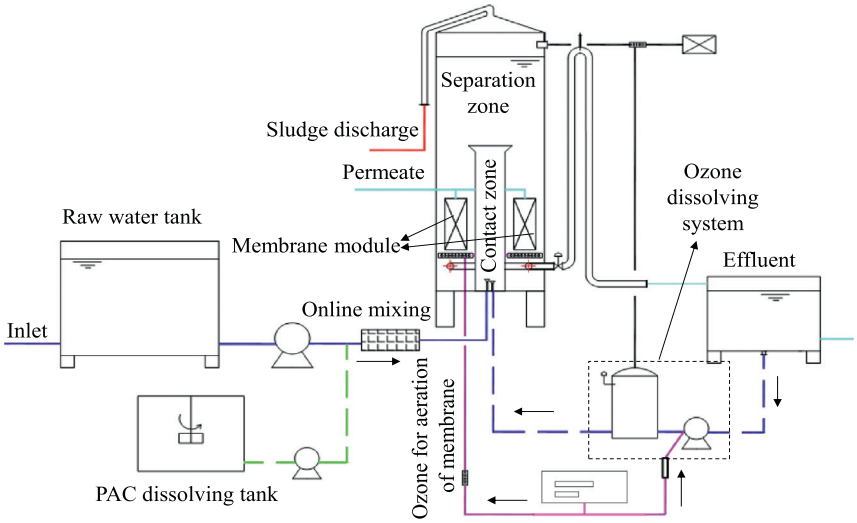

Fig. 1 – Experimental setup of MDOF process.

was operated at a pressure of 0.4 MPa. Appendix A Table S1 summarizes the standard operating conditions of the MDOF reactor.

During the operation of the MDOF reactor, the ozone dosage can be adjusted by changing the input power of the discharge tube of the ozone generator. In this study, 35% and 65% of the maximum input power was applied, which corresponds to 0.91 and 1.74 mg O_3/mg DOC, respectively (The raw water DOC was 7.899 ± 0.858 mg/L). The detailed ozone dosage calculation and measurements can be seen in the Appendix A Text. S1 and Table S2.

1.2. Raw water quality

The reactor was fed by the effluent from the sedimentation tank in a municipal wastewater treatment plant (WWTP) in Xi'an, China. The WWTP mainly treats domestic wastewater with a biological anaerobic–anoxic–oxic (AAO) treatment process. The raw water possessed the following characteristics: DOC = 7.899 ± 0.858 mg/L, UV_{254} = 0.119 ± 0.009 cm^{-1}, turbidity = 2.69 ± 0.99 NTU, pH 7.49 ± 0.17, alkalinity = 4.375 ± 0.220 mmol/L as HCO_3^-, NO_3-N = 0.159 ± 0.014 mg N/L, and chlorides = 216.53 ± 31.18 mg/L.

1.3. Analytical methods

1.3.1. Water quality analysis

Water quality parameters were monitored during the operation of the MDOF reactor. DOC was measured using a Shimadzu TOC_{VCPH} analyzer with an infrared detector. The DOC analyzer was calibrated with potassium hydrogen phthalate standard solutions before each run. All the samples were filtered with a 0.45-μm filter, acidified with H_2SO_4, and purged with nitrogen to remove inorganic carbon before measurement. UV_{254} was measured at 254 nm with a UV–VIS spectrophotometer (UV-4802 UNIC™, China) using 1-cm path-length quartz cells. Turbidity was measured using a turbidity meter (HI93703-1 HANNA, Italy). Total coliforms were measured according to the Chinese National Environmental Protection Agency (CNEPA) Standard Methods (CNEPA, 2002).

1.3.2. Cake sludge collection

The cake sludge formed on the membrane surface was scraped off with a plastic sheet when the flat sheet membrane was taken out from the MDOF reactor at the end of the experiments. The collected cake sludge was suspended in a certain volume of ultrapure water. The well-mixed diluted cake sludge sample was then used for the following analyses.

1.3.3. Extracellular polymeric substance (EPS) extraction and analysis

EPS extraction of the cake sludge sample was conducted according to the thermal treatment method (Hu et al., 2013). The analysis of the extracted EPS samples was carried out using the modified Lowry method for proteins (Hartree, 1972), using bovine serum albumin (BSA) as the standard, and using the phenol–sulfuric acid method for polysaccharides (Dubois et al., 1956), using glucose as the standard.

1.3.4. Particle size distribution analysis

The PSD of the cake sludge suspension was analyzed and compared using a laser granularity distribution analyzer (LS230/SVM$_+$, Beckman Coulter Corporation, USA) with a detection range of 0.4–2000 μm.

1.3.5. Molecular weight distribution analysis

The characterization of the apparent molecular weight distribution (MWD) of DOM in the MDOF process was performed using size exclusion chromatography (SEC) coupled with a UV detector. The detection wavelengths were 254 nm. The high-performance liquid chromatography (HPLC) system was a Shimadzu LC-2010AHF with a Zenix SEC-100 column (Sepax Technologies, USA). The injection volume was 20 μL, and the column temperature was 30°C. The mobile phase was a 150 mmol/L phosphate buffer solution (PBS) with a pH of 7.0 ± 0.1, and the flow rate was 0.8 mL/min.

1.3.6. Fouling layer morphology analysis

Small pieces of membrane were cut off with a sterile knife for analysis without damaging the structure of the cake layer from different positions of the membrane. A total of 1.5 μL/mL SYTO 9 (S34854, Molecular Probes®) and ConA (C860, Molecular Probes®) in MilliQ water was used to stain the samples in sequence. SYTO 9 was used to stain the nucleic acids of the cells, and ConA was used for polysaccharide staining. The staining process was done in the dark at room temperature for 30 min. Then, the samples were rinsed three times with MilliQ water to remove excess staining liquid before moving to the next staining probe.

The samples were immersed in MilliQ water prior to confocal laser scanning microscope (CLSM) analysis. The CLSMz-stack pictures of the stained biofilm samples were taken with a Leica SP8 confocal laser scanning microscope with a 10x objective (HCX PL APO CS 10x/0.40 Dry). SYTO 9 was excited with a 488 nm wavelength, and the emission wavelength was 500–550 nm. ConA was excited with a 550 nm wavelength, and the emission wavelength was 570–630 nm. A 1024 × 1024 image resolution was chosen, resulting in pixel size of 1.14 μm for image acquisition. The size of each image was 1.16 × 1.16 mm. Image analysis was conducted with an Image Structure Analyzer (ISA-2, Center for Biofilm Engineering-Montana State University) to obtain biofilm porosity and thickness data in the image stacks from samples taken from different positions of the membrane, and averaged results were obtained.

1.3.7. Three-dimensionalexcitation-emission matrix (3D-EEM) analysis

Fluorescence measurements were conducted using a spectrofluorometer (FP-6500, Jasco, Japan) with a 150 W xenon lamp. The analyses were performed at ambient temperature. A 1-cm quartz cuvette with four optical windows was used for the analyses. Emission scans were performed from 250 to 550 nm in 5 nm steps, while excitation wavelengths were measured from 200 to 450 nm at 2 nm intervals. The slit widths for excitation and emission were 5 nm. The detector was set to high sensitivity and the scanning speed was kept at 2000 nm/min. The fluorescence spectra for ultrapure water were measured using the same method and subtracted from all of the sample spectra to eliminate water Raman scattering and to reduce other background noise throughout the experimental period. The EEM spectra were plotted as contours. The X-axis represents the emission spectra, while the Y-axis represents the excitation wavelength, and the third dimension, *i.e.*, the contour line, is given to express the fluorescence intensity.

2. Results and discussion

2.1. Removal performance

The removal performance of the MDOF reactor fed by WWTP effluent is shown in Fig. 2. It can be seen from Fig. 2 that the

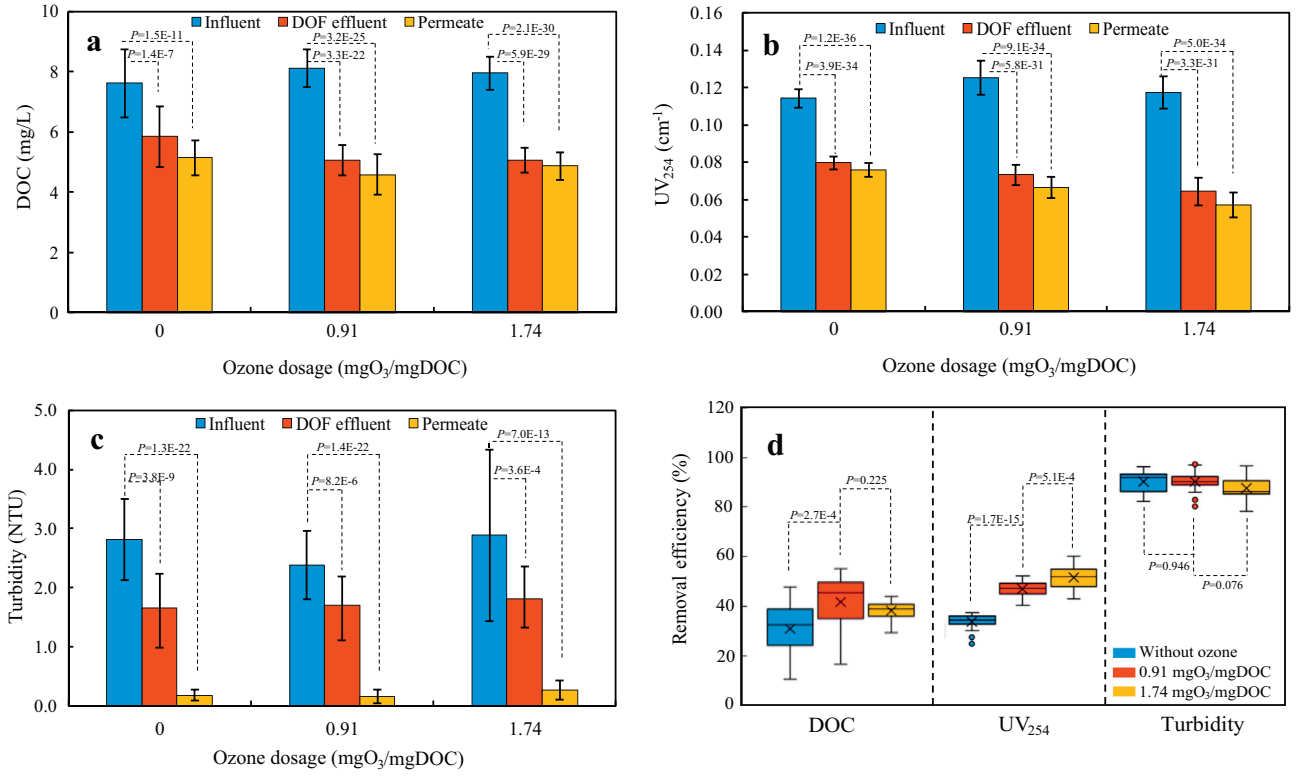

Fig. 2 – Removal performance for the treatment of WWTP effluent at different ozone dosages. (a) DOC; (b) UV_{254}; (c) turbidity removal performance; (d) total removal efficiency in the MDOF process.

DOC removal performance increased after addition of the ozone. However, with increasing ozone dosage, the DOC removal exhibited little variation. This is consistent with our previous study finding approximately 40% TOC removal efficiency using the DOF process in wastewater reclamation (Jin et al., 2006). Furthermore, the previous results also implied that TOC removal efficiency was enhanced compared to the DAF process (Jin et al., 2006). With increasing ozone dosage, the UV_{254} removal efficiency increased because of ozone addition. Ozone can react with unsaturated aromatic structures in organic matter, thus reducing UV_{254} (Chen et al., 2017; Gong et al., 2008). In the DOF reactor, ozonation and coagulation occurred simultaneously within a single reactor (Jin et al., 2006). Our previous study indicated that a metal coagulant in this process functions as catalyst to promote •OH generation in this kind of system and increases the removal efficiency of dissolved organic matter (Jin et al., 2017). Nevertheless, membrane filtration resulted in hardly any further removal of dissolved organic matter and UV_{254} according to Fig. 2. In the DOF part, part of the turbidity could be removed, and there was still some residual turbidity as shown in Fig. 2. Therefore, further separation processes were needed (Jin et al., 2016; Eades and Brignall, 1995). In this case, membrane filtration had superior and stable turbidity removal efficiency, and there was little effect of ozone dosage on the turbidity removal performance in the MDOF process.

2.2. Fouling behavior

Fig. 3 illustrates the flux curves at different ozone dosages during the operation of the MDOF reactor. The time-dependent flux profiles followed a similar "two-stage trend" (Peter-Varbanets et al., 2010). As shown in Fig. 3, the flux in the first stage decreased significantly in the first 30 days. In the second stage, the permeate flux remained stable at approximately 70, 60, and 55 L/(m^2 hr) for ozone dosages of 1.76, 0.91 and 0 mg O_3/mg DOC, respectively. Stabilization of the permeate flux was related to the development of a heterogeneous fouling layer adhered to the membrane surface (Derlon et al., 2013). According to Fig. 3, the addition of ozone could mitigate membrane fouling. Therefore, the MDOF process was more favorable for membrane filtration operation compared

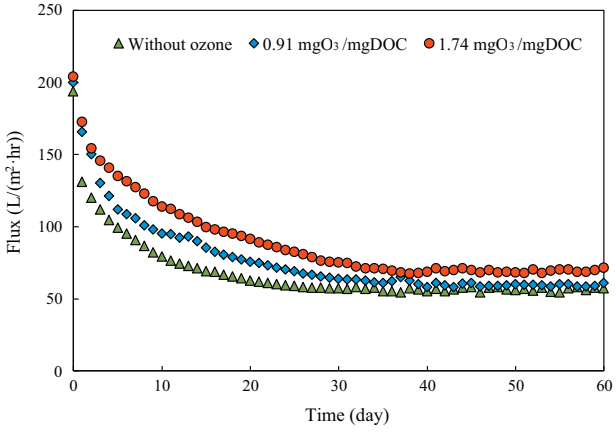

Fig. 3 – Flux decline at different ozone dosages.

with the MDAF process. Ozonation could completely mineralize some low MW organic molecules and/or partially decompose large molecules into hydrophilic and small-molecule substances, inducing less accumulation of organic matter on the membrane surface (Van Geluwe et al., 2011). Therefore, despite the higher energy cost of the MDOF process caused by the application of ozone, the operation cycle of MDOF process can be extended because of the mitigation of membrane fouling. Furthermore, the stabilized flux in this study was higher than that found in previous GDM research, which can be attributed to the much higher water level (2.0 m water level) compared with previous studies (Ding et al., 2018; Wang et al., 2017b; Shao et al., 2016). A previous study implied that higher hydrostatic pressure results in an increase in stable flux (Akhondi et al., 2015).

2.3. Characterization of dissolved organic matter in the MDOF process

Soluble microbial products (SMP) secreted by microorganisms during biological treatment processes, *e.g.*, humic-like substances and protein-like substances, are considered critical membrane foulants (Zheng et al., 2014). Fig. 4 shows the effect of ozone addition on the fluorescence characteristics of DOM in the MDOF process. Fig. 4 shows that only one notable fluorescent peak was observed, *i.e.*, Ex/Em 240/400 nm, which is identified as a fulvic-like substance (Pons et al., 2004). However, the fluorescence intensity exhibited little decrease without ozone addition because of the limited DOM removal performance in the MDAF process. With increasing ozone dosage, the peak intensity further decreased, and the peak location was blue-shifted. A blue-shift is associated with the decomposition of condensed aromatic moieties and the break-up of large molecules into smaller fragments (Coble, 1996; Korshin et al., 1999; Swietlik et al., 2004). Furthermore, many studies reported that high molecular weight organic matter can transform into low molecular weight organic matter during ozonation (Jin et al., 2016; Wert et al., 2011; Zhang et al., 2008). The addition of ozone to the membrane tank decreases the accumulation of organic matter retained on the membrane surface or in the membrane pores because of the increased hydrophilicity of smaller molecular weight organic matter (Yu et al., 2016a). Therefore, in this case, the MDOF process alleviates membrane fouling compared to the MDAF process. Appendix A Fig. S1 further confirms that the addition of ozone can transform large molecular weight organics into smaller molecular weight organics, which can also explain the blue-shift of fluorescence peaks in Fig. 4.

2.4. Characterization of the fouling layer

2.4.1. EPS contents of fouling layer

It has been suggested that membrane fouling can be generally regarded as the irreversible deposition of dissolved extracellular polymer substances (EPS), which are mainly composed of proteins and polysaccharides (Xue et al., 2016; Zheng et al., 2009; Yu et al., 2014, 2017). Fig. 5 represents the EPS concentration (proteins and polysaccharides) at the end of each run for different ozone dosages. Fig. 5 shows that the fouling layer (cake layer) was mainly composed of polysaccharides. This

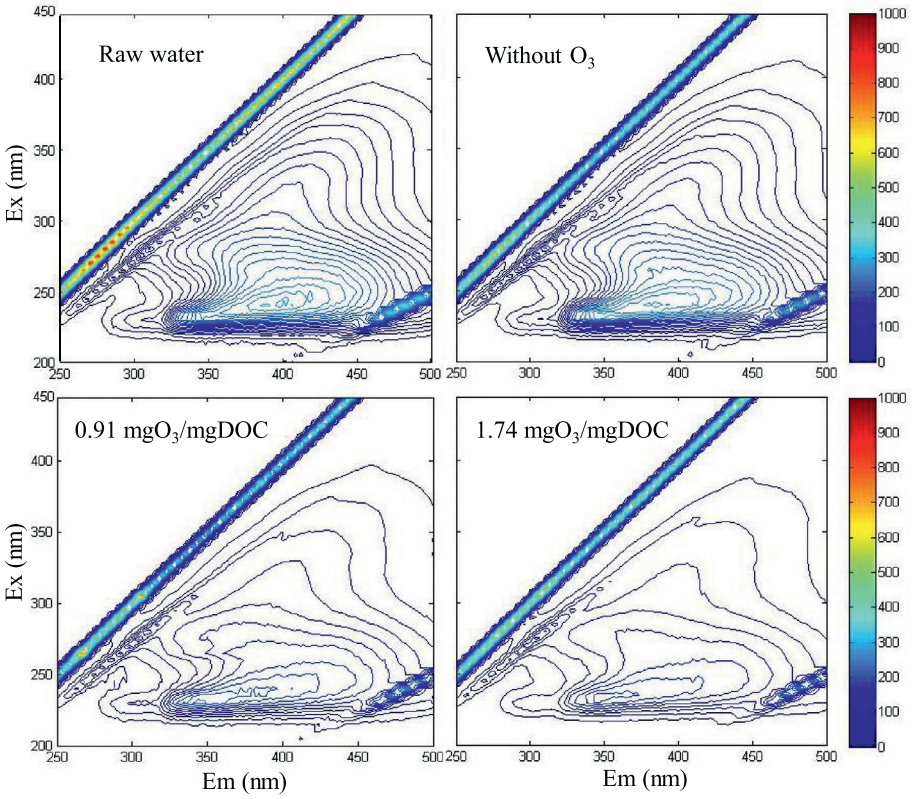

Fig. 4 – EEM spectra of DOM in MDOF process at different ozone dosages.

result was consistent with previous studies (Chang et al., 2015; Yu et al., 2016b). Some studies indicated that polysaccharides within the cake layer may be a key factor causing membrane fouling (Yu et al., 2014; Amy and Cho, 1999; Chon and Cho, 2016). In this case, coagulation was achieved in the MDOF reactor. It is believed that the higher concentration of proteins and polysaccharides in the cake layer enabled the coagulant flocs or particles (also containing EPS) to attach easily to the cake layer on the membrane surface, thereby forming a thicker cake layer (Yu et al., 2016b; Yu et al., 2014). Nevertheless, the addition of ozone decreased the EPS content. By increasing the ozone dosage, the EPS concentration in the cake layer further decreased. It has been reported that ozone is capable of degrading polysaccharides (Song et al., 2015) and proteins (Sharma, 2010). Therefore, it has been proposed that ozone can react with EPS, especially polysaccharides, to alleviate membrane fouling. It was revealed that ozone can decrease the concentration of EPS, particularly polysaccharides and proteins in the membrane cake layer (Yu et al., 2016a). The reduced EPS and bacterial concentrations resulted in a much thinner cake layer. It was found that the reduction of polysaccharide concentrations by pre-ozonation was statistically correlated with membrane fouling mitigation (Wang et al., 2017a). On the other hand, as EPS is produced by bacteria on the membrane surface, the quantity of total bacteria in the MDOF reactor was investigated, and the results are shown in Appendix A Fig. S2. Because of the powerful disinfection potential, the total bacteria count decreased, which also resulted in a reduction in the EPS concentration in the cake layer. Therefore, the reduction of EPS in the cake layer was attributed to both the direct reaction with ozone and a decrease in the total bacteria count.

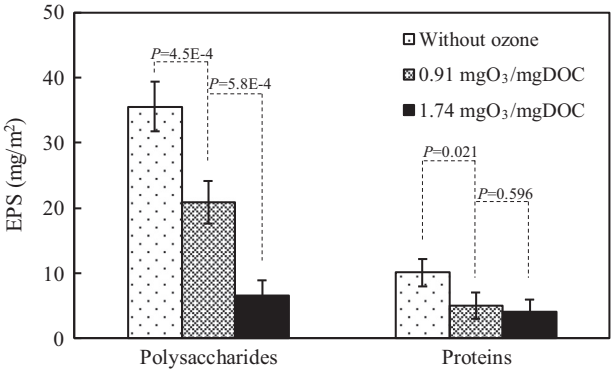

Fig. 5 – EPS contents of the fouling layer at different ozone dosages.

2.4.2. Fluorescence characteristics of EPS from the cake layer

EEM fluorescence spectra of EPS extracted from membrane foulants were also analyzed to further understand the fouling characteristics. As illustrated in Appendix A Fig. S3, three fluorescence peaks were observed, which were located at Ex/Em of 235/340, 250/435, and 275/330 nm. The peaks located at Ex/Em of 235/340 and 275/330 nm have been reported as

aromatic protein-like substances and tryptophan protein-like substances, respectively (Chen et al., 2003; Yamashita and Tanoue, 2003). Additionally, the peak at Ex/Em 250/435 nm was identified as fulvic-like substances (Pons et al., 2004). Three fluorescence peaks were also observed for the extracted EPS, and the fluorescence intensity decreased generally at an ozone dosage of 0.91 mg O_3/mg DOC in the MDOF process. The peaks located at Ex/Em of 235/375 and 275/340 nm both had red-shifts compared to the case without ozone. A red-shift is related to the presence of carbonyl-containing substituents, hydroxyl, alkoxyl, amino groups, and carboxyl constituents (Chen et al., 2002). Ozonation can lead to an increase in the amount of oxygen-containing groups such as carbonyl-containing groups, hydroxyl groups, and carboxyl groups, which can account for the red-shift of the two protein-like substances (Jin et al., 2016). Furthermore, XPS analysis also proves the increasing content of oxygen-containing groups in the extracted EPS (Appendix A Fig. S4). However, the peak at Ex/Em of 240/400 nm (fulvic-like substances) was blue-shifted compared to the case without ozone. When the ozone dosage increased to 1.74 mg O_3/mg DOC, only two fluorescence peaks were observed (*i.e.*, an Ex/Em of 235/350 and 245/430 nm). The peak at an Ex/Em of 235/350 nm (aromatic protein-like substances) was blue-shifted, while the peak at an Ex/Em of 245/430 nm (fulvic-like substances) was red-shifted. In addition, the fluorescence intensity of both peaks was further decreased. It is well known that the constituents of EPS, such as protein-like substances and humic-like substances, play an important role in membrane fouling (Wang et al., 2017b; Xue et al., 2016; Yu et al., 2016b, Yu et al., 2017; Lee et al., 2006). According to Appendix A Fig. S3, compared with the MDAF process, the MDOF process can remove or inhibit the formation of protein-like and fulvic-like substances in extracted EPS to mitigate membrane fouling.

2.4.3. Particle size distribution in the cake layer

Particle size is important since this determines, to a major degree, the nature of interactions between EPS and the UF membrane (Yu et al., 2017). The interactions can be in the form of a cake layer, pore blocking, or the adsorption/accumulation of organic matter within the membrane pores. It is likely that serious membrane fouling will be caused if the particle size is close to the diameter of the membrane pores. In contrast, particles that are significantly smaller than, or larger than, the pore size, are unlikely to induce significant membrane fouling (Yu et al., 2017). It was also reported that the aggregation of particles can alleviate membrane fouling due to pore blocking and irreversible fouling (Abdelrasoul et al., 2017). Appendix A Fig. S5 represents the particle size distribution of the fouling layer. It can be seen that the particle size increased with increasing ozone dosage, both in terms of mean size and distribution. Because of their size, the larger particles that formed had little impact on the membrane pores in this case (0.1 μm), and they formed a relatively porous cake layer on the surface of the membrane. This finding can explain the mitigation of membrane fouling with the application of ozonation. It has been reported that ozonation can increase the amount of oxygen-containing functional groups such as hydroxyl and carboxyl groups of dissolved organic matter (Jin et al., 2016). Moreover, aluminum in the coagulant can easily complex with hydroxyl or carboxyl groups on organic matter to form aggregates (Song et al., 2015), which results in larger particle sizes in the cake layer and higher flux with ozone addition.

2.4.4. Morphology of the fouling layer

To further analyze membrane fouling in the MDOF process, the fouling layer morphology was examined *via* CLSM. The 3D reconstruction images of the fouling layer at different ozone dosages are shown in Fig. 6. The size of each image is 1.16 × 1.16 mm. The green and red colors represent bacterial cells and polysaccharides, respectively. Fig. 6 shows that the membrane surface was unevenly covered by foulants with different thicknesses and with varying morphology. According to Fig. 6, the fouling layer thickness generally decreases with increasing ozone dosage. The calculated average biovolume is shown in Appendix A Fig. S6. Moreover, the biovolume of the foulants decreased significantly after addition of ozone in the MDOF process. In addition, the average porosity of membrane foulants increased with increasing ozone dosage. According to previous studies (Cheng et al., 2016; Huang et al., 2018; Yu et al., 2016a), much thinner cake layers were also observed after the addition of ozone. Two possible reasons could explain this (Yu et al., 2016b). On the one hand, when ozone was added to the membrane tank, the lower EPS content results in less EPS passing through the cake layer and onto the surface of membrane. On the other hand, the nature of organic matter dissolved in the membrane tank changed markedly from hydrophobic to hydrophilic as a result of ozone addition, thereby inducing less organic matter to be adsorbed on the membrane surface.

The porosity distribution along the membrane foulant thickness is also shown in Fig. 6. Moving from the surface of membrane to the bulk phase, the porosity first decreased and then increased with three different ozone dosages. The same phenomenon was also obtained by previous studies (Hwang et al., 2012, Hwang et al., 2007; Hong et al., 2007). The membrane foulant attached to the membrane surface at the very early initial stage may have a loose structure, whereas the bio-cakes formed by cohesion might be more tightly compacted than the membrane foulants formed by adhesion from the membrane surface to 50–100 μm. This could explain why the porosity of the cake layer decreased as the depth increased (Hwang et al., 2007). Furthermore, bacterial cells and polysaccharides in the upper part of the cake layer would have a greater propensity to slough and back-transport to the bulk phase than those inside the cake layer. Therefore, the porosity increased as the cake layer approached the bulk phase (Hwang et al., 2007).

2.5. Membrane fouling mitigation mechanism

Size exclusion is widely recognized as a core mechanism of UF membrane filtration. Substances such as polysaccharides and proteins that are close to the membrane pore size can cause pore blockages that severely increase filtration resistance, while substances much larger than membrane pores lead to cake formation (Lohwacharin and Takizawa, 2009). The addition of ozone in the MDOF process can transform large MW organics into smaller fragments. Much research has also

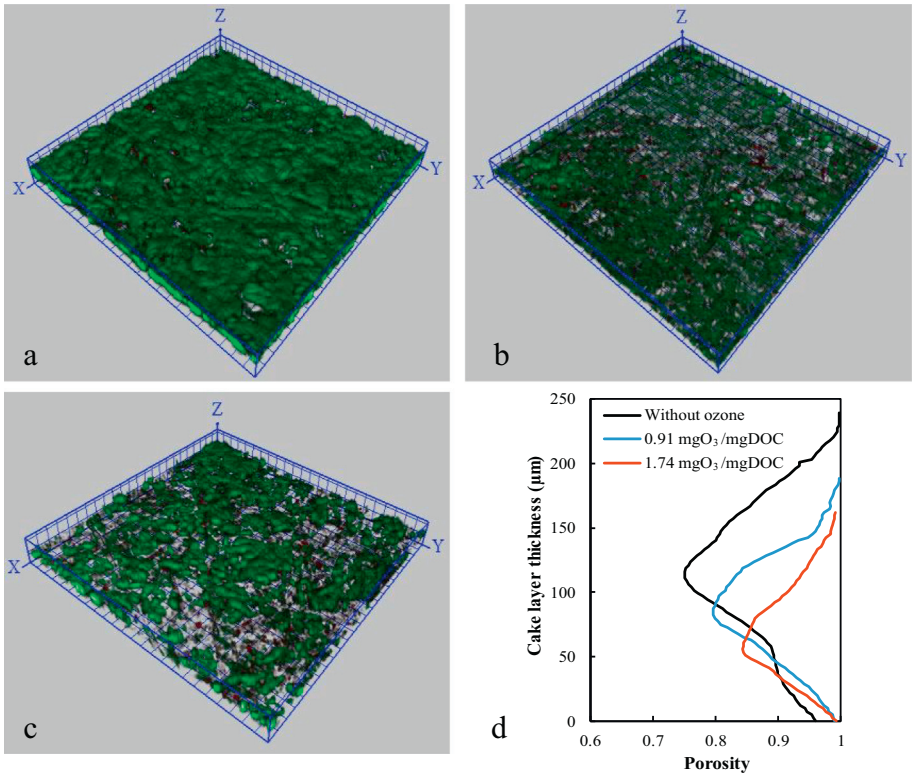

Fig. 6 – CLSM 3D image of fouling layer and porosity distribution along the cake layer thickness at different ozone dosages. (a) 0 mg O_3/mg DOC; (b) 0.91 mg O_3/mg DOC; (c) 1.74 mg O_3/mg DOC; (d) porosity distribution.

confirmed that pre-ozonation can decompose organic molecules into smaller fragments, which are more hydrophilic (Cheng et al., 2016; Van Geluwe et al., 2011). Additionally, hydrophilic reaction products formed through pre-ozonation exhibit a lower propensity for adsorption onto membrane surfaces (Cheng et al., 2016). Furthermore, several studies have applied *in situ* ozonation to mitigate membrane fouling (Song et al., 2017; Song et al., 2018; Tang et al., 2018). Compared with pre-ozonation, *in situ* ozonation significantly improved mitigation performance for hydraulically irreversible fouling, which was attributed to the oxidation of foulants accumulated on the membrane surface and in the membrane pores (Song et al., 2017). The generation of hydroxyl radicals during ozonation can further enhance oxidation of the accumulated foulants on the membrane surface and within the membrane pores (Song et al., 2017). Furthermore, the existence of chlorides in the WWTP effluent can also work as adjuvant for the foulants oxidation (Monteagudo et al., 2016; Gomes et al., 2019). At the same time, coagulation has been shown to be an effective and low-cost approach for reducing membrane fouling because of the removal of macro-organic matter and bacteria by coagulation (Yu et al., 2016a; Kimura et al., 2014). However, in this study, the mechanism of membrane fouling mitigation in the MDOF process is somewhat different from that in previous studies. The proposed membrane fouling mitigation mechanism is shown in Fig. 7. In the MDOF process, coagulation and *in situ* ozonation occurred simultaneously in one reactor. Besides the *in situ* ozonation and coagulation in the MDOF process for membrane fouling mitigation, according to our previous work (Jin et al., 2017), Al-based coagulants can act as a catalyst to enhance the decomposition of ozone and generate more hydroxyl radicals compared with ozonation alone, which is the reason why membrane fouling in the MDOF process can be better alleviated compared to the MDAF process.

3. Conclusions

A novel integrated membrane filtration and DOF (MDOF) process was proposed in this study. Membrane filtration in the MDOF process further enhances the turbidity removal performance. Membrane filtration in the MDOF process was operated in a gravity-driven mode. The MDOF process differs from the conventional process of pre-ozonation before membrane filtration, in that *in situ* ozonation occurred in the MDOF process because ozonation, coagulation, and filtration occurred in a single reactor. Under the operating conditions, membrane fouling was mitigated in the MDOF process compared with that in the MDAF process. *In situ* ozonation in the MDOF process can decrease the fluorescence intensity and transform high MW dissolved organics into lower MW organics. In addition, the EPS contents of the cake layer significantly decreased in the MDOF process. The addition of ozone also resulted in a thinner and more loosely structured cake layer. Moreover, coagulation and ozonation occurred simultaneously in a single reactor in the MDOF process. Al-based coagulants can act as catalysts to enhance the

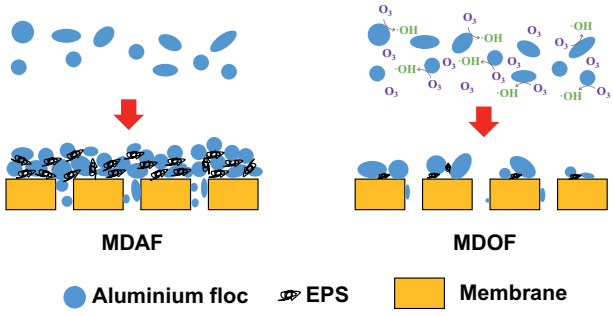

Fig. 7 – Membrane mitigation mechanism in the MDOF process.

decomposition of ozone to generate more hydroxyl radicals compared with ozonation alone. Therefore, membrane fouling can be better alleviated in the MDOF process compared to the MDAF process.

Acknowledgments

This work was supported by the National Natural Science Foundation of China (No. 51708443), the National Key Research and Development Program of China (No. 2016YFC0400701), the China Postdoctoral Science Foundation (No. 2017M623326XB) and the Shaanxi Provincial Department of Education Key Laboratory Research Projects (No. 18JS057).

Appendix A. Supplementary data

Supplementary data to this article can be found online at https://doi.org/10.1016/j.jes.2019.02.011.

REFERENCES

Abdelrasoul, A., Doan, H., Lohi, A., Cheng, C.H., 2017. The influence of aggregation of latex particles on membrane fouling attachments & ultrafiltration performance in ultrafiltration of latex contaminated water and wastewater. J. Environ. Sci. 52, 118–129.

Akhondi, E., Wu, B., Sun, S., Marxer, B., Lim, W., Gu, J., et al., 2015. Gravity-driven membrane filtration as pretreatment for seawater reverse osmosis: linking biofouling layer morphology with flux stabilization. Water Res. 70, 158–173.

Amy, G., Cho, J., 1999. Interactions between natural organic matter (NOM) and membranes: rejection and fouling. Water Sci. Technol. 40, 131–139.

C.N.E.P.A. CNEPA, 2002. Water and Wastewater Monitoring Methods. 4th Ed. Chinese Environmental Science Publishing House, Beijing, China.

Chang, H., Qu, F., Liu, B., Yu, H., Kai, L., Shao, S., et al., 2015. Hydraulic irreversibility of ultrafiltration membrane fouling by humic acid: effects of membrane properties and backwash water composition. J. Memb. Sci. 493, 723–733.

Chen, J., Gu, B., Leboeuf, E.J., Pan, H., Dai, S., 2002. Spectroscopic characterization of the structural and functional properties of natural organic matter fractions. Chemosphere 48, 59–68.

Chen, J., LeBoeuf, E.J., Dai, S., Gu, B., 2003. Fluorescence spectroscopic studies of natural organic matter fractions. Chemosphere 50, 639–647.

Chen, Z., Li, M., Wen, Q., Ren, N., 2017. Evolution of molecular weight and fluorescence of effluent organic matter (EfOM) during oxidation processes revealed by advanced spectrographic and chromatographic tools. Water Res. 124, 566–575.

Cheng, X., Liang, H., An, D., Qu, F., Shao, S., Liu, B., et al., 2016. Effects of pre-ozonation on the ultrafiltration of different natural organic matter (NOM) fractions: membrane fouling mitigation, prediction and mechanism. J. Memb. Sci. 505, 15–25.

Chon, K., Cho, J., 2016. Fouling behavior of dissolved organic matter in nanofiltration membranes from a pilot-scale drinking water treatment plant: an autopsy study. Chem. Eng. J. 295, 268–277.

Coble, P.G., 1996. Characterization of marine and terrestrial DOM in seawater using excitation–emission matrix spectroscopy. Mar. Chem. 51, 325–346.

Derlon, N., Koch, N., Eugster, B., Posch, T., Pernthaler, J., Pronk, W., et al., 2013. Activity of metazoa governs biofilm structure formation and enhances permeate flux during gravity-driven membrane (GDM) filtration. Water Res. 47, 2085–2095.

Ding, A., Wang, J., Lin, D., Zeng, R., Yu, S., Gan, Z., et al., 2018. Effects of GAC layer on the performance of gravity-driven membrane filtration (GDM) system for rainwater recycling. Chemosphere 191, 253–261.

Dubois, M., Gilles, K.A., Hamilton, J.K., Rebers, P.A., Smith, F., 1956. Colorimetric method for determination of sugars and related substances. Anal. Chem. 28, 350–356.

Eades, A., Brignall, W.J., 1995. Counter-current dissolved air flotation/filtration. Water Sci. Technol. 31, 173–178.

Edzwald, J.K., 2010. Dissolved air flotation and me. Water Res. 44, 2077–2106.

Fortunato, L., Jeong, S., Wang, Y., Behzad, A.R., Leiknes, T., 2016. Integrated approach to characterize fouling on a flat sheet membrane gravity driven submerged membrane bioreactor. Bioresour. Technol. 222, 335–343.

Gomes, J.F., Lopes, A., Gmurek, M., Quinta-Ferreira, R.M., Martins, R.C., 2019. Study of the influence of the matrix characteristics over the photocatalytic ozonation of parabens using Ag-TiO_2. Sci. Total Environ. 646, 1468–1477.

Gong, J., Liu, Y., Sun, X., 2008. O_3 and UV/O_3 oxidation of organic constituents of biotreated municipal wastewater. Water Res. 42, 1238–1244.

Huang, H., Schwab, K., Jacangelo, J.G., 2009. Pretreatment for low pressure membranes in water treatment: a review. Environ. Sci. Technol. 43, 3011–3019.

Hartree, E.F., 1972. Determination of protein: a modification of the Lowry method that gives a linear photometric response. Anal. Biochem. 48, 422–427.

Hong, S.H., Lee, W.N., Oh, H.S., Yeon, K.M., Hwang, B.K., Lee, C.H., et al., 2007. The effects of intermittent aeration on the

characteristics of bio-cake layers in a membrane bioreactor. Environ. Sci. Technol. 41, 6270–6276.
Hu, Y., Wang, X.C., Zhang, Y., Li, Y., Chen, H., Jin, P., 2013. Characteristics of an A^2O-MBR system for reclaimed water production under constant flux at low TMP. J. Memb. Sci. 431, 156–162.
Hwang, B.K., Lee, W.N., Park, P.K., Lee, C.H., Chang, I.S., 2007. Effect of membrane fouling reducer on cake structure and membrane permeability in membrane bioreactor. J. Memb. Sci. 288, 149–156.
Hwang, B.K., Lee, C.H., Chang, I.S., Drews, A., Field, R., 2012. Membrane bioreactor: TMP rise and characterization of biocake structure using CLSM-image analysis. J. Memb. Sci. 419-420, 33–41.
Jin, P.K., Wang, X.C., Hu, G., 2006. A dispersed-ozone flotation (DOF) separator for tertiary wastewater treatment. Water Sci. Technol. 53, 151–157.
Jin, X., Jin, P.K., Wang, X.C., 2015. A study on the effects of ozone dosage on dissolved-ozone flotation (DOF) process performance. Water Sci. Technol. 71, 1423–1428.
Jin, P.K., Xin, J., Bjerkelund, V.A., Østerhus, S.W., Wang, X.C., Lei, Y., 2016. A study on the reactivity characteristics of dissolved effluent organic matter (EfOM) from municipal wastewater treatment plant during ozonation. Water Res. 88, 643–652.
Jin, X., Jin, P., Hou, R., Yang, L., Wang, X.C., 2017. Enhanced WWTP effluent organic matter removal in hybrid ozonation-coagulation (HOC) process catalyzed by Al-based coagulant. J. Hazard. Mater. 327, 216–224.
Kim, J., Shan, W., Davies, S.H.R., Baumann, M.J., Masten, S.J., Tarabara, V.V., 2009. Interactions of aqueous NOM with nanoscale TiO_2: implications for ceramic membrane filtration-ozonation hybrid process. Environ. Sci. Technol. 43, 5488–5494.
Kimura, K., Tanaka, K., Watanabe, Y., 2014. Microfiltration of different surface waters with/without coagulation: clear correlations between membrane fouling and hydrophilic biopolymers. Water Res. 49, 434–443.
Korshin, G.V., Kumke, M.U., Li, C.W., Frimmel, F.H., 1999. Influence of chlorination on chromophores and fluorophores in humic substances. Environ. Sci. Technol. 33, 1207–1212.
Lee, B.H., Kim, S.H., Kim, S.H., 2004. DOF (dissolved ozone flotation) technology in wastewater treatment. Proceedings of the 8th Russian-Korean International Symposium on Science and Technology, pp. 331–333.
Lee, W.N., Kang, I.J., Lee, C.H., 2006. Factors affecting filtration characteristics in membrane coupled moving bed biofilm reactor. Water Res 40, 1827–1835.
Lee, W., Lee, H.W., Choi, J.S., Oh, H.J., 2014. Effects of transmembrane pressure and ozonation on the reduction of ceramic membrane fouling during water reclamation. Desalin. Water Treat. 52, 612–617.
Lohwacharin, J., Takizawa, S., 2009. Effects of nanoparticles on the ultrafiltration of surface water. J. Memb. Sci. 326, 354–362.
Ma, J., Fu, K., Lei, D., Jiang, L., Guan, Q., Zhang, S., et al., 2017. Flocculation performance of cationic polyacrylamide with high cationic degree in humic acid synthetic water treatment and effect of kaolin particles. Sep. Purif. Technol. 181, 201–212.
Monteagudo, J.M., Durán, A., Latorre, J., Expósito, A.J., 2016. Application of activated persulfate for removal of intermediates from antipyrine wastewater degradation refractory towards hydroxyl radical. J. Hazard. Mater. 306, 77–86.
Peter-Varbanets, M., Hammes, F., Vital, M., Pronk, W., 2010. Stabilization of flux during dead-end ultra-low pressure ultrafiltration. Water Res. 44, 3607–3616.
Pons, M.N., Le Bonté, S., Potier, O., 2004. Spectral analysis and fingerprinting for biomedia characterisation. J. Biotechnol. 113, 211–230.
Shao, S., Feng, Y., Yu, H., Li, J., Liang, H., Li, G., 2016. Presence of an adsorbent cake layer improves the performance of gravity-driven membrane (GDM) filtration system. Water Res. 108, 240–249.
Sharma, V.K., 2010. Oxidation of amino acids, peptides, and proteins. Ozone Sci. Eng. 32, 81–90.
Song, A., Xiang, L., Yan, L., Lyu, L., Ma, L., 2015. Fate of organic pollutants in a full-scale drinking water treatment plant using O_3-BAC. Ozone Sci. Eng. 37, 257–268.
Song, S., Zhang, Z., Zhang, X., 2017. A comparative study of pre-ozonation and in-situ ozonation on mitigation of ceramic UF membrane fouling caused by alginate. J. Memb. Sci. 538, 50–57.
Song, J., Zhang, Z., Tang, S., Tan, Y., Zhang, X., 2017. Does pre-ozonation or in-situ ozonation really mitigate the protein-based ceramic membrane fouling in the integrated process of ozonation coupled with ceramic membrane filtration? J. Memb. Sci. 548, 254–262.
Swietlik, J., Dabrowska, A., Raczyk-Stanislawiak, U., Nawrocki, J., 2004. Reactivity of natural organic matter fractions with chlorine dioxide and ozone. Water Res. 38, 547–558.
Szymanska, K., Zouboulis, A.I., Zamboulis, D., 2014. Hybrid ozonation–microfiltration system for the treatment of surface water using ceramic membrane. J. Memb. Sci. 468, 163–171.
Tang, S., Zhang, Z., Zhang, X., 2018. Coupling in-situ ozonation with ferric chloride addition for ceramic ultrafiltration membrane fouling mitigation in wastewater treatment: quantitative fouling analysis. J. Memb. Sci. 555, 307–317.
Geluwe, S.V., Braeken, L., Bruggen, B.V.D., 2011. Ozone oxidation for the alleviation of membrane fouling by natural organic matter: a review. Water Res. 45, 3551–3570.
Wang, H., Park, M., Liang, H., Wu, S., Lopez, I.J., Ji, W., et al., 2017a. Reducing ultrafiltration membrane fouling during potable water reuse using pre-ozonation. Water Res. 125, 42–51.
Wang, Y., Fortunato, L., Jeong, S., Leiknes, T.O., 2017b. Gravity-driven membrane system for secondary wastewater effluent treatment: filtration performance and fouling characterization. Sep. Purif. Technol. 184, 26–33.
Wang, W., Yue, Q., Li, R., Bu, F., Shen, X., Gao, B., 2018. Optimization of coagulation pre-treatment for alleviating ultrafiltration membrane fouling: the role of floc properties on Al species. Chemosphere 200, 86–92.
Wert, E.C., Sarah, G., Mei, D.M., Rosario-Ortiz, F.L., 2011. Evaluation of enhanced coagulation pretreatment to improve ozone oxidation efficiency in wastewater. Water Res. 45, 5191–5199.
Wu, B., Hochstrasser, F., Akhondi, E., Ambauen, N., Tschirren, L., Burkhardt, M.N., et al., 2016. Optimization of gravity-driven membrane (GDM) filtration process for seawater pretreatment. Water Res. 93, 133–140.
Wu, B., Christen, T., Tan, H.S., Hochstrasser, F., Suwarno, S.R., Liu, X., et al., 2017. Improved performance of gravity-driven membrane filtration for seawater pretreatment: implications of membrane module configuration. Water Res. 114, 59–68.
Huang, X., Gao, B., Yue, Q., Wang, Y., Li, Q., 2018. Effects of polytitanium chloride and polyaluminum chloride pre-treatment on ultrafiltration process: floc properties and membrane fouling. J. Taiwan Inst. Chem. Eng. 88, 193–200.
Xue, J., Zhang, Y., Liu, Y., Eldin, M.G., 2016. Effects of ozone pretreatment and operating conditions on membrane fouling behaviors of an anoxic-aerobic membrane bioreactor for oil sands process-affected water (OSPW) treatment. Water Res. 105, 444–455.
Yamashita, Youhei, Tanoue, Eiichiro, 2003. Chemical characterization of protein-like fluorophores in DOM in relation to aromatic amino acids. Mar. Chem. 82, 255–271.
Yu, W., Xu, L., Graham, N., Qu, J., 2014. Pre-treatment for ultrafiltration: effect of pre-chlorination on membrane fouling. Sci. Rep. 4 (6513), 1–8.
Yu, W., Graham, N.J.D., Fowler, G.D., 2016a. Coagulation and oxidation for controlling ultrafiltration membrane fouling in drinking water treatment: application of ozone at low dose in submerged membrane tank. Water Res. 95, 1–10.
Yu, W., Yang, Y., Graham, N., 2016b. Evaluation of ferrate as a coagulant aid/oxidant pretreatment for mitigating submerged

ultrafiltration membrane fouling in drinking water treatment. Chem. Eng. J. 298, 234–242.
Yu, W., Zhang, D., Graham, N.J.D., 2017. Membrane fouling by extracellular polymeric substances after ozone pre-treatment: variation of nano-particles size. Water Res. 120, 146–155.
Zhang, T., Lu, J., Ma, J., Qiang, Z., 2008. Comparative study of ozonation and synthetic goethite-catalyzed ozonation of individual NOM fractions isolated and fractionated from a filtered river water. Water Res. 42, 1563–1570.
Zhang, X., Guo, J., Wang, L., Hu, J., Zhu, J., 2013. In situ ozonation to control ceramic membrane fouling in drinking water treatment. Desalination 328, 1–7.
Zheng, X., Ernst, M., Jekel, M., 2009. Identification and quantification of major organic foulants in treated domestic wastewater affecting filterability in dead-end ultrafiltration. Water Res. 43, 238–244.
Zheng, X., Khan, M.T., Croué, J.P., 2014. Contribution of effluent organic matter (EfOM) to ultrafiltration (UF) membrane fouling: isolation, characterization, and fouling effect of EfOM fractions. Water Res. 65, 414–424.